REGULAR CONTRIBUTED PAPER

WILEY

Improved stability in organic light-emitting devices by mixing ambipolar and wide energy gap hosts

John S. Bangsund[1] | Kyle W. Hershey[1] | Dominea C. K. Rathwell[3] |
Hong-Yeop Na SID Member[3] | Jeong-Hwan Jeon[3] | Peter Trefonas[2] |
Russell J. Holmes[1]

[1] Department of Chemical Engineering
and Materials Science, University of
Minnesota, Minneapolis, Minnesota, USA

[2] DuPont Electronics and Imaging,
Marlborough, Minnesota, USA

[3] DuPont Seoul Technology Center,
Hwaseong, Gyeonggi-Do, Korea

Correspondence
Russell J. Holmes, Department of
Chemical Engineering and Materials
Science, University of Minnesota,
Minneapolis, MN 55455.
Email: rholmes@umn.edu

Abstract

We demonstrate improved stability in phosphorescent organic light-emitting devices (OLEDs) by incorporating a wide energy gap host material into an ambipolar emissive layer. Unlike conventional mixed-host OLEDs that combine hole- and electron-transporting hosts, charge transport in this device occurs primarily along the ambipolar host and the emitter, while the wide energy gap host serves to modify the charge injection and transport characteristics of the emissive layer. This approach allows both the width and position of the exciton recombination zone to be tuned without introducing exciplex states. Whereas overall device stability improves with increasing recombination zone width in conventional mixed-host OLEDs, mixing in this system reduces the recombination zone extent yet still increases device lifetime. By decoupling luminance losses into the photostability of the emitter and the exciton formation efficiency, we show that this enhancement arises from a trade-off between bulk and interfacial degradation. The addition of the wide energy gap host moves the recombination zone away from the interface between the hole-transport layer and the emissive layer, sacrificing a modest increase in bulk degradation to substantially reduce interfacial degradation. We find that the lifetime can be improved by 50% by balancing these competing degradation pathways.

1 | INTRODUCTION

Several studies of operational stability in organic light-emitting devices (OLEDs) have suggested that exciton density-driven processes are responsible for overall device degradation.[1–5] Consequently, substantial work has sought to reduce exciton density in the OLED emissive layer (EML) by engineering the exciton recombination zone (RZ). The RZ is the spatial extent of exciton formation in an OLED, and its width determines the exciton

density for a given luminance, setting the rate of EML degradation.[2,6] Previous studies have found that device lifetime can be enhanced by maximizing the RZ width.[2,6–8] In conventional mixed- and graded-EML devices, electron- and hole-transporting hosts are mixed to achieve high charge balance and a wide RZ.[7,9–13] The absolute position of the RZ is also important, as proximity to a transport layer interface can exacerbate degradation,[14–17] or influence exciton confinement and charge balance.[17–19] In cases showing interfacial degradation, the RZ is typically pinned at the degrading interface. Avoiding both bulk and interface degradation suggests a trade-off between increased RZ width for reduced exciton

---

John S. Bangsund and Kyle W. Hershey contributed equally to this work.

density and the need to avoid stressing unstable interfaces.

In this work, we demonstrate an unconventional mixed-EML approach to improve device stability that combines an ambipolar charge-transporting host with a wide energy gap host. The use of a wide-energy gap host as an additive provides an advantage of simplifying the host pair selection process. A wide-gap host is less likely to act as a charge trap or introduce an exciplex state, which could change the exciton formation mechanism, quench the emitter excitons or introduce unwanted spectral features. Varying the EML composition permits tuning of the exciton RZ width and position, and an optimization of device stability. This system illustrates a trade-off between bulk and interfacial degradation as lifetime is not optimized for devices with the broadest RZ, in contrast to conventional mixed-EML OLEDs.[20–22] It is further interesting to note that the stability of an ambipolar host material can be enhanced through the addition of a wide energy gap host, which modulates charge transport and the RZ in the EML.

Here, devices are constructed using two proprietary host materials supplied by DuPont Electronics and Imaging, designated host A and host B. While we cannot disclose the chemical structures of these host materials, we provide characterization of the molecular energy levels and optical and electrical properties of both host A and host B, which should allow these results to be reproduced in other materials systems displaying similar properties. In commercial devices manufactured by DuPont Electronics and Imaging, devices based on a uniform host mixture show improved lifetimes up to t_{90}=8.6 hours (ie, the time to 90% of initial luminance) at an initial luminance of L_0 = 15 000 cd/m^2, compared with t_{90}=1.3 hours and t_{90}=4.2 hours for devices containing only host A or host B, respectively. It is worth noting that these lifetimes are reported at an extreme luminance condition used for rapid commercial screening.

Figure 1A shows the molecular orbital energy levels for the active materials of interest. The highest occupied molecular orbital (HOMO) energy levels for TCTA, TPBi, and Ir(ppy)$_3$ are obtained from literature ultraviolet photoelectron spectroscopy (UPS) measurements.[23,24] The HOMO levels for host A and host B were calculated from the oxidation potential in cyclic voltammetry (CV) measurements and corrected using established relationships between CV and UPS measurements.[23] The lowest unoccupied molecular orbital (LUMO) levels of TCTA and Ir(ppy)$_3$ are taken
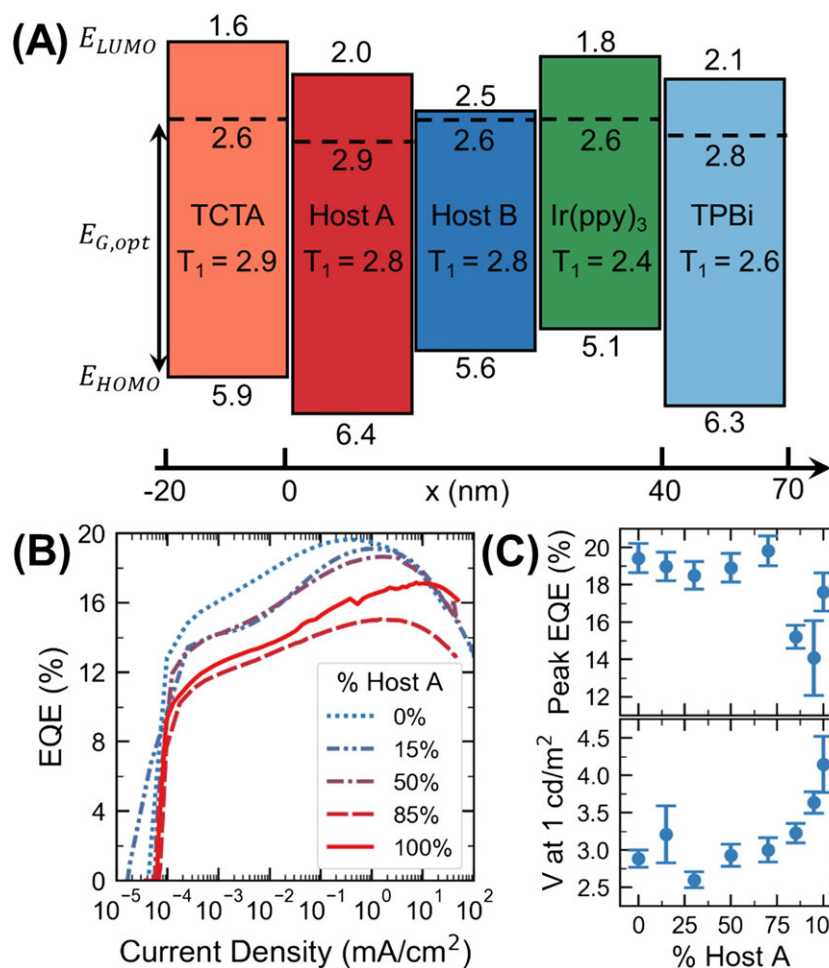

FIGURE 1 A, Energy level schematic showing the highest occupied molecular orbital (HOMO), lowest unoccupied molecular orbital (LUMO), and triplet energy levels for the materials used in this study. The dashed line indicates the optical energy gap relative to the HOMO level. The x-axis denotes the layer thicknesses used in the devices of interest, as a function of distance from the hole-transport layer(HTL)/emissive layer (EML) interface. B, External quantum efficiency (EQE) as a function of current density for various EML compositions. (c) Peak EQE and turn-on voltage (at 1 cd/m^2) as a function of percent host A in the EML (ignoring emitter concentration). Error bars represent standard deviations taken over at least four separate pixels

from literature inverse photoelectron spectroscopy (IPES) measurements,[25] while all others are calculated from the reduction potential in CV measurements, and again corrected using prior work comparing CV and IPES measurements.[26] The optical energy gaps for each material are shown in Figure 1A as dashed lines relative to the HOMO level ($E_g = 3.5$ eV for host A and $E_g = 3.0$ eV for host B, Figure S1). The triplet energy levels (labeled T_1) are also shown in Figure 1A. The triplet energy levels for host A and host B were estimated from low temperature phosphorescence (Figure S1), while those for the other materials were taken from literature.[27–30] Despite having differences in energy gap and fluorescence energy, host A and host B have similar triplet energies. It is worth noting that the energy levels of host B reside entirely within those of host A, and hosts A and B do not form an emissive exciplex, as confirmed from measurements of mixed film photoluminescence (PL) and bilayer device (ITO/host A/host B/LiF/Al) electroluminescence (EL).

The dependence of the external quantum efficiency (EQE) and driving voltage on EML composition is shown in Figure 1B and 1C. Relative to a device with an EML of host B and Ir(ppy)$_3$, the addition of the wide energy gap host A has minimal impact on EQE at moderate concentrations, only leading to a reduction in efficiency at compositions greater than 70% host A (defined relative to the total host composition). Likewise, the turn-on voltage to achieve 1 cd/m^2, shown in Figure 1C, is relatively constant up to 70% host A. The power efficiency at 1000 cd/m^2 is minimally impacted over this range, decreasing slightly from (37 ± 1) lm/W for 0% host A to (34 ± 2) lm/W for 50% host A (**Figure S2**). As host A composition is increased above 70%, the turn-on voltage increases from approximately 3 V to approximately 4.2 V, leading to a corresponding decrease in power efficiency to (25 ± 4) lm/W. This increase in turn-on voltage is attributed to a reduction in the efficiency of charge injection and transport upon adding host A to the EML, reflecting, in part, the difference in molecular orbital energy levels.

Figure 2 shows the dependence of device lifetime on EML composition, with mixed architectures showing superior stability to those based on single-host EMLs containing only one of the hosts and Ir(ppy)$_3$. Interestingly, the stability of devices based on host B ($t_{80} = (40 \pm 2)$ hours), is improved upon adding host A ($t_{80} = (59 \pm 2)$ hours for an EML containing a 1:1 mixture of the two hosts), despite devices based on an EML of host A:Ir(ppy)$_3$ showing a short lifetime ($t_{80} = 7$ hours). In contrast, the degradation in PL efficiency is slowest for devices with an EML of host B:Ir(ppy)$_3$ ($t_{95} = (48 \pm 10)$ hours), with mixed host devices showing faster PL degradation (Figure 2B). In previous work, PL stability has been found to scale with exciton density, with devices having the widest RZ
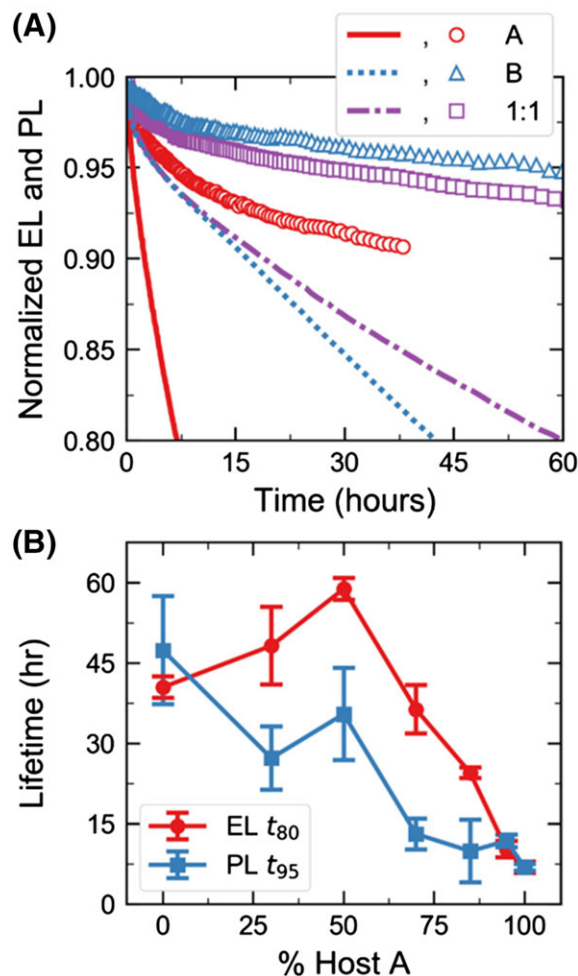

FIGURE 2 A, Normalized electroluminescence (EL, lines) and photoluminescence (PL, symbols) decay curves for devices having an emissive layer (EML) consisting of host A, host B, or a uniform mixture of host A and host B (1:1). The initial luminance is 5000 cd/m^2 in all cases, with an operating current density of approximately 8 mA/cm^2. B, EL lifetime (time to reach 80% of initial value, t_{80}) and PL lifetime (t_{95}) as a function of percent host A in the EML (ignoring emitter concentration). EL lifetime is maximized at a host composition of 50% host A, whereas the PL lifetime is longest at a host composition of 100% host B. Error bars represent standard deviations taken over at least four separate pixel lifetimes

showing the longest PL lifetime.[2] Here, this suggests that the RZ is widest in devices containing an EML of host B: Ir(ppy)$_3$, yet that the overall EL lifetime is not optimized by maximizing RZ width. This observation may indicate that RZ position changes with composition, leading to a trade-off between bulk degradation within the EML and interface degradation adjacent to the EML.[14–16] To test this hypothesis, the RZ is measured directly.

The RZ for devices containing 0%, 50%, and 100% host B (defined relative to the total host composition) were measured using a δ-doped sensitizer approach.[31] Discontinuous layers (nominally 0.1-nm thick) of the near-infrared phosphor Pt (II) tetraphenyltetrabenzoporphyrin

(PtTPTBP) were deposited at various locations in the EML. Thin, discontinuous strips are used to limit concentration quenching and minimize the impact of the sensitizer on the electrical properties of the device. Excitons residing on Ir(ppy)$_3$ within a Förster radius of the sensitizer (R$_0$ = 3.7 nm, see **Figure S3**) are quenched, leading to emission from PtTPTBP and a reduction in the intensity of Ir(ppy)$_3$ emission. The ratio of EL from Ir(ppy)$_3$ between sensitized and control devices (denoted β) reflects the fraction of electrically generated excitons, which are not quenched by the sensitizer, ie, which recombine on Ir(ppy)$_3$ molecules more than a Förster radius away from the sensitizer strip. Therefore, $(1 - \beta)$ reflects the local exciton density quenched by the sensitizer strip.[32] By translating this sensitizer across the EML, $(1 - \beta)$ reflects the relative exciton population profile across the EML. This measurement is found to agree within error with RZ probes based off of an out-coupling corrected sensitizer EL approach.[2,18,33] The area-normalized exciton population map resulting from this measurement for each architecture is shown in Figure 3A, with the associated EL spectra included in **Figure S4**. Devices based on an EML of host A have the highest exciton density of all three architectures, with a narrow RZ peaked at the electron-transport layer (ETL) interface. Those based on an EML of host B show the widest RZ; that is, nearly flat across the EML. The uniform mixture EML device shows an intermediate behavior with a narrower RZ than Host B that is also shifted away from the hole-transport layer (HTL)/EML interface.

The shift in RZ width and position can be understood by considering how the addition of host A to the EML changes injection and charge transport. Both injection and transport are assessed in single-carrier devices fabricated for compositions of 0%, 50%, and 100% host B. The current density-voltage characteristics for hole-only (HOD) and electron-only (EOD) devices are shown in Figure 3B and 3C. In both cases, devices based on host B show larger currents than those based on host A. The addition of host A to host B reduces both the hole- and electron-currents, suggesting host B and the phosphorescent guest remain the dominant transporting phase, even in mixtures. Thus, the observed shift in device stability and RZ position reflect a favorable adjustment in the transport properties of the EML upon adding host A. These results, taken together with the RZ measurements, indicate that adding host A to the EML serves to preferentially frustrate the transport and injection of electrons in the EML. While host A also impacts hole transport, the net impact is to reduce the electron concentration in the EML and shift the RZ towards the EML/ETL interface.

The trend in measured RZ width is consistent with expectations based on the PL stability behavior in
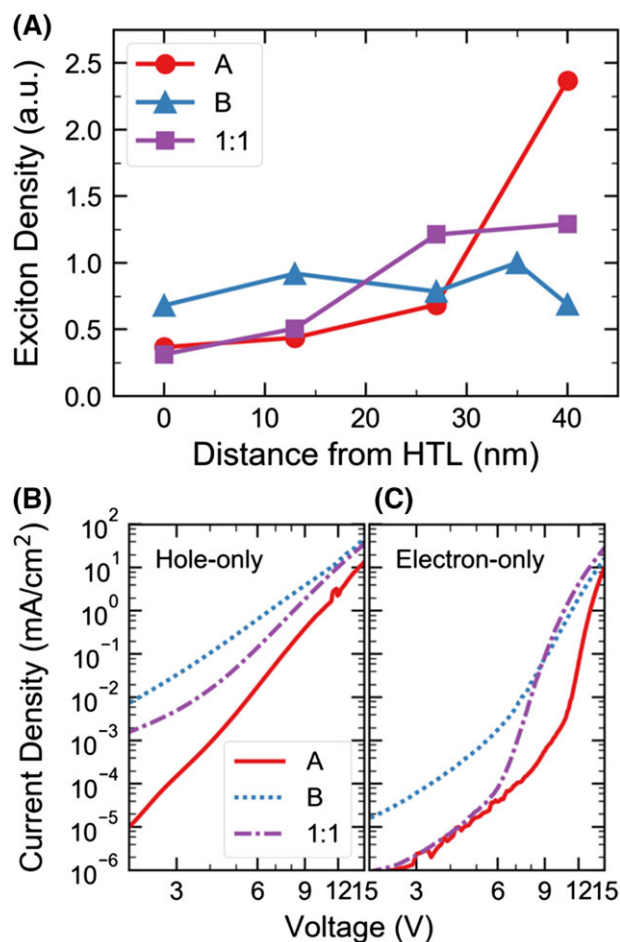

FIGURE 3 A, Area-normalized exciton density profiles extracted from electroluminescence spectra of devices with δ-doped exciton quenching layers. The host B device shows the broadest recombination zone (RZ), whereas the host A device shows an RZ pinned at the emissive layer (EML)/electron-transport layer (ETL) interface. The uniform, 1:1 mixture of host A and host B shows intermediate behavior and has a reduced exciton density at the hole-transport layer (HTL)/EML interface. B, Current density-voltage characteristics for hole-only devices and C, electron-only devices with EMLs consisting of host A, host B, and a uniform mixture of host A and host B

Figure 2B, where a narrower RZ leads to greater exciton density and directly accelerates PL degradation. The observed increase in the overall EL stability of the mixture, despite its reduced RZ width and PL stability, suggests that the EL stability is limited by the position of the RZ. Specifically, the exciton density in the 100% host B device is only higher than the uniform mixture near the HTL/EML interface. This suggests that the HTL/EML interface is sensitive to exciton density and limits the overall stability of the wide RZ, 100% host B device.

To further confirm that the lifetime enhancement upon mixing is driven by reduced interfacial degradation and not differences in intrinsic or morphological stability

of the EML, devices were fabricated with a 10-nm-thick EML. A thin EML helps to minimize variations in RZ position and width between devices, making more uniform the role of degradation at the HTL/EML interface. For these devices, the ETL thickness is increased to 50 nm to center the electric field profile of the $\lambda = 473$ nm pump laser in the EML (**Figure S5**). All other layers have the same thicknesses as the 40-nm-thick EML devices. The peak EQE of these devices is $(14 \pm 1)\%$ for all three EML architectures (**Figure S6**). The EL and PL lifetimes for devices operated at an initial luminance of 5000 cd/m^2 are shown in Figure 4. Devices with an EML containing host B and a 1:1 mixture of host A and host B are found to have nearly identical lifetimes with EL $t_{80} = (3.1 \pm 0.3)$ hours for host B and $t_{80} = (3.4 \pm 0.4)$ hours for the mixture, and PL $t_{95} = (0.6 \pm 0.1)$ hours for host B and $t_{95} = (0.9 \pm 0.4)$ hours for the mixture. This behavior suggests that the intrinsic and/or morphological stability is the same for devices based on host B and the uniform mixture, providing further evidence that stability differences for the 40-nm-thick EML devices stem from differences in RZ position. Devices containing an EML of host A:Ir(ppy)$_3$ still show a shorter lifetime in both EL and PL, likely because of the narrow RZ of these devices, which is heavily peaked at the ETL interface.

Taken together with the RZ measurements, these thin EML device results indicate that the HTL/EML interface is sensitive to exciton density and limits the overall stability of the 100% host B device. This interfacial exciton sensitivity is likely because of an accumulated density of polarons at the interface, leading to exciton-polaron annihilation driven degradation processes, such as host or transport layer aggregate formation, as have been reported previously.[14,15] The addition of host A to the EML moves the RZ away from this interface in 40-nm-thick EML devices, reducing the exciton density at this interface and increasing the EL stability. It is worth noting that the ETL/EML interface can also contribute to degradation, and degradation at this interface could limit stability in other materials systems. In these cases, we expect that a wide energy gap host, which selectively frustrates hole transport and injection would provide similar stability improvements. In a general sense, this approach could improve the reliability of existing host materials that have desirable properties but are limited by nonoptimum RZ profiles. Importantly, this method does not require a reengineering of transport and blocking layers or the development of entirely new materials to realize the desired RZ. Use of a wide-gap host is advantageous since it is less likely to act as a charge trap or introduce an exciton state, which could change the exciton formation mechanism, quench the emitter, or introduce unwanted spectral features. In this way, a wide gap host can tune the mobility and RZ of a device without impacting the emission spectrum or the exciton formation mechanism. From a design perspective, the wide-gap host should have a deeper HOMO and shallower LUMO than the other host and emitter, preventing charge trapping or exciplex formation, and addition of the wide-gap host to the EML at low to moderate concentrations should have minimal impact on turn-on voltage.

In this work, increased device lifetime is demonstrated in an unconventional mixed-host architecture that combines wide energy gap and ambipolar hosts. Based on measurements of the exciton RZ, the wide energy gap host serves to frustrate electron injection and transport in the EML, allowing the position and width of the RZ to be controlled. Notably, lifetime is improved upon mixing despite a reduction in both RZ width and PL stability. The overall increase in stability is shown to result from shifting the RZ away from an unstable interface. This work offers a new strategy to manage the position of the RZ, allowing device lifetime to be optimized by balancing the trade-off between bulk and interfacial degradation.
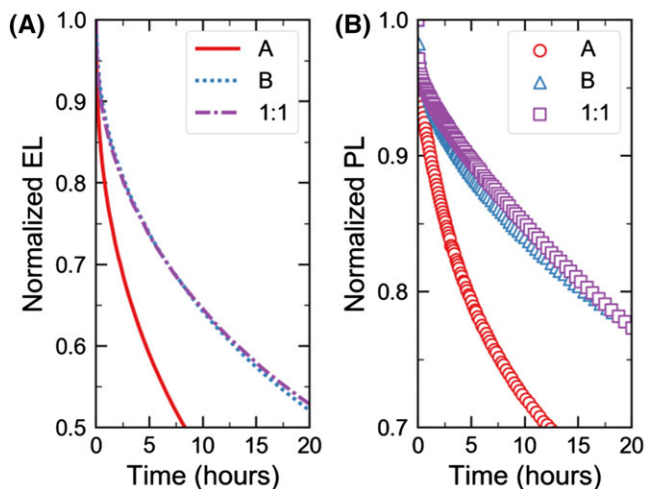

FIGURE 4 Normalized A, electroluminescence (EL) and B, photoluminescence (PL) decays for devices with a 10-nm-thick emissive layer (EML) operated at an initial luminance of 5000 cd/m^2. Devices consisting of host B and a uniform mixture show identical EL and PL lifetimes, indicating that when differences in recombination zone (RZ) position and width are reduced, the stability of these two devices is identical

2 | EXPERIMENTAL SECTION

2.1 | Device fabrication

Devices with an active area of 25 mm^2 were fabricated on glass substrates prepatterned with a 150-nm-thick anode layer of indium tin oxide (ITO, Xinyan). Substrates were

cleaned with solvents followed by exposure to ambient UV-ozone. A hole-injection layer of poly (thiophene-3-[2[(2-methoxyethoxy)ethoxy]-2,5-diyl) (AQ1250, Sigma Aldrich) was spin-cast on the ITO anode, followed by an HTL of 4,4′,4″-tris(N-carbazolyl)triphenylamine (TCTA, TCI America). The EML consists of host A, host B, or a mixture of the two hosts, and a constant emitter loading of 15 vol.% fac-tris(2-phenylpyridine)iridium (III) (Ir(ppy)₃, Lumtec). The remaining 85 vol.% of the EML consisted of mixture compositions of 0%, 5%, 15%, 30%, 50%, 70%, 85%, and 100% host A by volume. An ETL of tris-(1-phenyl-1H-benzimidazole) (TPBi, Lumtec, sublimed grade) is deposited over the EML, followed by a 1 nm LiF/100 nm Al cathode. The full device architecture was: ITO/AQ1250 (70 nm)/TCTA (20 nm)/EML (40 nm)/TPBi (30 nm) /LiF (1 nm)/Al (100 nm). The HIL is spin-cast in a N_2 glovebox and annealed for 30 minutes at 150°C. The remaining layers are deposited by vacuum thermal evaporation at a base pressure $< 7 \times 10^{-7}$ Torr and a rate of 0.3 nm/s. Devices are encapsulated with epoxy and a cover glass in a N_2 glovebox. PtTPTBP, used for RZ sensing experiments, was purchased from Frontier Scientific.

2.2 | Single-carrier device architectures

The layer structure for EOD is ITO (150 nm)/Al (10 nm)/LiF (1 nm)/TPBi (20 nm)/EML (100 nm)/TPBi (20 nm)/LiF (1 nm)/Al (100 nm). The layer structure for HOD is ITO (150 nm)/AQ1250 (70 nm)/TCTA (20 nm)/EML (100 nm)/TCTA (20 nm)/MoO$_x$ (10 nm)/Al (100 nm). All EMLs were doped with 15 vol.% Ir(ppy)₃.

2.3 | Device efficiency and stability characterization

Efficiency and luminance measurements were taken with an Agilent 4155C parameter analyzer and a large area photodiode (Hamamatsu S3584–08), assuming Lambertian emission for luminance calculations. EL spectra were collected with an Ocean Optics HR4000 spectrometer. Unless otherwise noted, device lifetimes were characterized at an initial luminance of 5000 cd/m² using a Keithley 26XX to source device current and to measure device EL from a Hamamatsu S2281 photodiode. PL was measured periodically during degradation by temporarily removing the current and optically pumping the device using a $\lambda = 473$ nm laser (Coherent OBIS). The PL signal was passed through a 500-nm long pass filter to prevent detection of stray laser light. This method has been previously described and has been shown to introduce no further degradation to devices or influence the electrical lifetime.[16]

2.4 | CV measurements

Hosts A and B were dissolved in N,N-dimethylformamide at a concentration of approximately 1 mM, with 0.1 M tetrabutylammonium tetrafluoroborate as the supporting electrolyte. A Pt counter electrode, Pt working electrode with an area of 0.3 mm², and an Ag/Ag⁺ reference electrode were used, and measurements were calibrated with a ferrocene standard. TPBi was measured in acetonitrile.

ORCID

John S. Bangsund 🔟 https://orcid.org/0000-0001-6666-4190
Hong-Yeop Na 🔟 https://orcid.org/0000-0001-8668-2062
Jeong-Hwan Jeon 🔟 https://orcid.org/0000-0002-1893-0447
Peter Trefonas 🔟 https://orcid.org/0000-0002-4538-9588
Russell J. Holmes 🔟 https://orcid.org/0000-0001-7183-3673

REFERENCES

1. Giebink NC et al. Intrinsic luminance loss in phosphorescent small-molecule organic light emitting devices due to bimolecular annihilation reactions. J. Appl. Phys. 2008;103:044509.

2. Bangsund JS, Hershey KW, Holmes RJ. Isolating degradation mechanisms in mixed emissive layer organic light-emitting devices. ACS Appl. Mater. Interfaces. 2018;10:5693–5699. https://doi.org/10.1021/acsami.7b16643

3. Kondakov DY. Organic Electronics Materials, Processing, Devices and Applications. In: So F, The Role of Homolytic Reactions in the Instrinsic Degradation of OLEDs. Boca Raton, FL, USA: CRC Press, 2010; p. 211–242.

4. Schmidbauer S, Hohenleutner A, König B. Chemical degradation in organic light-emitting devices: mechanisms and implications for the design of new materials. Adv. Mater. 2013;25:2114–2129.

5. Scholz S, Kondakov D, Lüssem B, Leo K. Degradation mechanisms and reactions in organic light-emitting devices. Chem. Rev. 2015;115:8449–8503.

6. Zhang Y, Lee J, Forrest SR. Tenfold increase in the lifetime of blue phosphorescent organic light-emitting diodes. Nat. Commun. 2014;5:1–7.

7. Chwang AB, Kwong RC, Brown JJ. Graded mixed-layer organic light-emitting devices. Appl. Phys. Lett. 2002;80:725–727.

8. Wu Z et al. Achieving extreme utilization of excitons by an efficient sandwich-type emissive layer architecture for reduced efficiency roll-off and improved operational stability in organic light-emitting diodes. ACS Appl. Mater. Interfaces. 2016;8:3150–3159.

9. Erickson NC, Holmes RJ. Relating charge transport and performance in single-layer graded-composition organic light-emitting devices. J. Appl. Phys. 2011;110:084515.

10. Lee S et al. The role of charge balance and excited state levels on device performance of exciplex-based phosphorescent organic light emitting diodes. Sci. Rep. 2017;7:11995.

11. Lee J-H, Wu C-I, Liu S-W, Huang C-A, Chang Y. Mixed host organic light-emitting devices with low driving voltage and long lifetime. Appl. Phys. Lett. 2005;86:103506.

12. Hsiao C-HC-C, Chen Y-H, Lin T-C, Hsiao C-HC-C, Lee J-H. Recombination zone in mixed-host organic light-emitting devices. Appl. Phys. Lett. 2006;89:163511.

13. Song W, Lee JY, Cho YJ, Yu H, Aziz H, Lee KM. Electroplex as a new concept of universal host for improved efficiency and lifetime in red, yellow, green, and blue phosphorescent organic light-emitting diodes. Adv. Sci. 2018;5:1700608.

14. Wang Q, Sun B, Aziz H. Exciton–Polaron-induced aggregation of wide-bandgap materials and its implication on the electroluminescence stability of phosphorescent organic light-emitting devices. Adv. Funct. Mater. 2014;24:2975–2985.

15. Wang Q, Aziz H. Degradation of organic/organic interfaces in organic light-emitting devices due to polaron-exciton interactions. ACS Appl. Mater. Interfaces. 2013;5:8733–8739.

16. Hershey KW, Suddard-Bangsund J, Qian G, Holmes RJ. Decoupling degradation in exciton formation and recombination during lifetime testing of organic light-emitting devices. Appl. Phys. Lett. 2017;111:113301.

17. Jeon SK, Lee JY. Four times lifetime improvement of blue phosphorescent organic light-emitting diodes by managing recombination zone. Org Electron Phys Mater Appl. 2015;27:202–206.

18. Coburn C, Lee J, Forrest SR. Charge balance and exciton confinement in phosphorescent organic light emitting diodes. Adv Opt Mater. 2016;4:889–895.

19. Coburn C, Forrest SR. Effects of charge balance and exciton confinement on the operational lifetime of blue phosphorescent organic light-emitting diodes. Phys Rev Appl. 2017;7:041002.

20. Kim J-M, Lee C-H, Kim J-J. Mobility balance in the light-emitting layer governs the polaron accumulation and operational stability of organic light-emitting diodes. Appl. Phys. Lett. 2017;111:203301.

21. Shin H et al. Blue phosphorescent organic light-emitting diodes using an exciplex forming co-host with the external quantum efficiency of theoretical limit. Adv. Mater. 2014;26:4730–4734.

22. Yamada Y, Inoue H, Mitsumori S, et al. 52-4: achievement of blue phosphorescent organic light-emitting diode with high efficiency, low driving voltage, and long lifetime by exciplex—triplet energy transfer technology. SID Symp. Dig. Tech. Pap. 2016;47:711–714.

23. D'Andrade BW, Datta S, Forrest SR, Djurovich P, Polikarpov E, Thompson ME. Relationship between the ionization and oxidation potentials of molecular organic semiconductors. Org Electron. 2005;6:11–20.

24. D'Andrade BW, Holmes RJ, Forrest SR. Efficient organic electrophosphorescent white-light-emitting device with a triple doped emissive layer. Adv. Mater. 2004;16:624–628.

25. Yoshida H, Yoshizaki K. Electron affinities of organic materials used for organic light-emitting diodes: a low-energy inverse photoemission study. Org. Electron. 2015;20:24–30.

26. Djurovich PI, Mayo EI, Forrest SR, Thompson ME. Measurement of the lowest unoccupied molecular orbital energies of molecular organic semiconductors. Org. Electron. 2009;10:515–520.

27. Turro N, Scaiano JC, Ramamurthy V. *Modern Molecular Photochemistry of Organic Molecules*University Science Books; 1991.

28. Goushi K, Kwong R, Brown JJ, Sasabe H, Adachi C. Triplet exciton confinement and unconfinement by adjacent hole-transport layers. J. Appl. Phys. 2004;95:7798–7802.

29. Goushi K, Kawamura Y, Sasabe H, Adachi C. Unusual phosphorescence characteristics of Ir(ppy)3 in a solid matrix at low temperatures. Jpn J Appl Phys Part 2 Lett. 2004;43:0–3.

30. Volcker A. Near-infrared phosphorescence emission of compounds with low-lying triplet states. Chem Phys Lett. 1989;159:103–108.

31. Sim B, Moon C-K, Kim K-H, Kim J-J. Quantitative analysis of the efficiency of OLEDs. ACS Appl. Mater. Interfaces. 2016;8:33010–33018.

32. Erickson NC, Holmes RJ. Engineering efficiency roll-off in organic light-emitting devices. Adv. Funct. Mater. 2014;24:6074–6080.

33. Lee J et al. Hot excited state management for long-lived blue phosphorescent organic light-emitting diodes. Nat. Commun. 2017;8:15566.

AUTHOR BIOGRAPHIES

John S. Bangsund is pursuing a PhD in Materials Science from the University of Minnesota. Since starting his graduate studies in 2015, his work has focused on understanding organic light-emitting device stability, particularly by quantifying the components of efficiency loss with optical techniques.
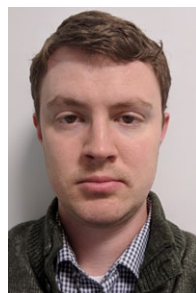
Kyle Hershey graduated from Coe College in 2013 with studies in Physics, Mathematics, and Computer Science. He completed his PhD in 2018 at the University of Minnesota under Prof Russell J. Holmes. His primary areas of study were transient OLED dynamics and operational lifetime. The title of his thesis is Multi-scale Dynamics of Organic Light Emitting Devices. He has since moved on to pursue opportunities as a Display Engineer at Microsoft.

Dominea Rathwell received her PhD in Organic Chemistry from the University of Auckland in 2009 and did postdoctoral research with Professor Seeberger at the Max Plank Institute for Colloids and Interfaces as a Humboldt Research Fellow. Since 2013, she has been engaged in the development of organic under layers and display chemicals at the electronic materials divisions of Samsung SDI, The Dow Chemical Company and presently at DuPont Electronics and Imaging.
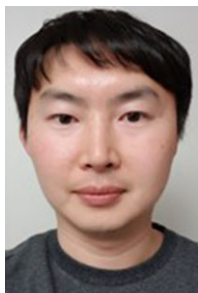
Hong-Yeop Na joined Gracel in 2006 after graduating from Sejong University with a bachelor's degree in Physics. Since then, he has researched the development of OLED materials and the device modification of fluorescent blue, phosphorescent red, electron transport, TADF and solution materials at Rohm and Haas and The Dow Chemical Company. He is currently conducting a study of OLED device fundamentals as a Sr. Engineer at DuPont Electronics and Imaging.

Jeong-Hwan Jeon received his MS in Chemistry from Kyunghee University in 2007 where he studied physical and computational chemistry. He has worked in OLED simulation modeling and device engineering at Gracel, Rohm and Haas, The Dow Chemical Company and most currently at DuPont Electronics and Imaging.

Peter Trefonas received his PhD in Chemistry from the University of Wisconsin-Madison in 1985 where he studied inorganic, polymer and photo chemistry. He has worked in the fields of simulation modeling, photoresists, organic antireflectant coatings and display chemicals at the electronic chemicals divisions of Monsanto Company, Aspect Systems, Shipley Company, Rohm and Haas, The Dow Chemical Company and most currently at DuPont Electronics and Imaging.

Russell J. Holmes received his PhD in Electrical Engineering from Princeton University in 2006 where he worked on blue organic electrophosphorescence and light-matter interactions in organic microcavities. After graduating, he joined the faculty of the Department of Chemical Engineering and Materials Science at the University of Minnesota. His research group specializes in the characterization of organic semiconductor thin films, as well as their application in optoelectronic devices.

SUPPORTING INFORMATION

Additional supporting information may be found online in the Supporting Information section at the end of the article.

How to cite this article: Bangsund JS, Hershey KW, Rathwell DCK, et al. Improved stability in organic light-emitting devices by mixing ambipolar and wide energy gap hosts. *J Soc Inf Display*. 2019;1–8. https://doi.org/10.1002/jsid.761